Available online at www.sciencedirect.com
ScienceDirect
Bioorganic & Medicinal Chemistry 14 (2006) 8073–8085
Bioorganic & Medicinal Chemistry

Synthesis and evaluation of α-hydroxymethylated conjugated nitroalkenes for their anticancer activity: Inhibition of cell proliferation by targeting microtubules

Renu Mohan,[a] Namrata Rastogi,[b] Irishi N. N. Namboothiri,[b,*] Shaikh M. Mobin[c] and Dulal Panda[a,*]

[a]*School of Biosciences and Bioengineering, Indian Institute of Technology, Bombay, Mumbai 400 076, India*
[b]*Department of Chemistry, Indian Institute of Technology, Bombay, Mumbai 400 076, India*
[c]*National Single Crystal X-ray Diffraction Facility, Indian Institute of Technology, Bombay, Mumbai 400 076, India*

Received 22 June 2006; revised 18 July 2006; accepted 19 July 2006
Available online 7 August 2006

Abstract—The Morita–Baylis–Hillman (MBH) type reaction of a variety of aromatic and heteroaromatic conjugated nitroalkenes with formaldehyde in the presence of stoichiometric amounts of imidazole and catalytic amounts (10 mol %) of anthranilic acid at room temperature provided the corresponding hydroxymethylated derivatives in moderate to good yield. The parent nitroalkenes and their MBH adducts were subsequently screened for their anticancer activity. Some of the MBH adducts were found to inhibit cervical cancer (HeLa) cell proliferation at low micromolar concentrations with half-maximal inhibitory concentrations in the range of 1–2 μM. The antiproliferative activity of 3-((*E*)-2-nitrovinyl)furan and three potent MBH adducts, namely, hydroxymethylated derivatives of 3-((*E*)-2-nitrovinyl)thiophene, 1-methoxy-4-((*E*)-2-nitrovinyl)benzene, and 1,2-dimethoxy-4-((*E*)-2-nitrovinyl)benzene was correlated well with their antimicrotubule activity. At their effective concentration range, the tested compounds perturbed the organization of mitotic spindle microtubules and chromosomes. In the presence of hydroxymethylated nitroalkenes, abnormal bipolar or multipolar mitotic spindles were apparent. Interphase microtubules were found to be significantly depolymerized at relatively higher concentrations of the tested compounds. These compounds inhibited tubulin assembly into microtubules in vitro by binding to tubulin at a site distinct from the vinblastine and colchicine binding sites. The compounds reduced the intrinsic tryptophan fluorescence of tubulin and the fluorescence of tubulin-1-anilinonaphthalene-8-sulfonic acid (ANS) complex indicating that they induced conformational changes in the tubulin. The results suggest that hydroxymethylated nitroalkenes exert their antiproliferative activity at least in part by depolymerizing cellular microtubules through tubulin binding and indicate that hydroxymethylated nitroalkenes are promising lead compounds for cancer therapy.

1. Introduction

Nitro compounds are versatile substrates by virtue of the ability of the nitro group to undergo a variety of useful synthetic transformations, such as conversion to 1,3-dipoles, primary alkyl radicals, oxidation to carboxylic acids, reduction to oximes, hydroxylamines or amines, to name a few.[1] A double bond activated by a nitro group is an excellent electrophile and conjugate additions of various C-, N-, O- and S-centered nucleophiles to nitroalkenes are well documented in the literature.[2] Nitro compounds, particularly conjugated nitroalkenes, also constitute an important class of compounds that has been extensively studied for its biological activity.[3] The pesticidal,[4] fungicidal,[5] and molluscicidal[6] activities of many aromatic and heteroaromatic nitroalkenes have been reported. Besides their own ability to behave as phosphate ester mimics,[7] diuretic agents,[8] and other bioactive materials,[9] nitroalkenes are useful intermediates in the synthesis of drugs, for example, antiulcer ranitidine and nizatidine,[10] and other bioactive natural products.[11]

Despite their distinct synthetic utility and biological activity, many potentially useful chemical and biological properties of conjugated nitroalkenes remain unexplored. For instance, the Morita–Baylis–Hillman

Keywords: Conjugated nitroalkenes; Microtubules; HeLa cell proliferation; Depolymerization.
* Corresponding authors. Tel.: +91 22 2576 7838; fax: +91 22 2572 3480; e-mail addresses: panda@iitb.ac.in; irishi@iitb.ac.in

0968-0896/$ - see front matter © 2006 Elsevier Ltd. All rights reserved.
doi:10.1016/j.bmc.2006.07.035

(MBH) reaction, that is, the coupling of activated alkenes with electrophiles such as aldehydes, imines, etc. in the presence of a tertiary amine or tertiary phosphine as catalyst,[12] has emerged as an elegant multicomponent and atom economical reaction in organic synthesis.[13,14] However, conjugated nitroalkenes are conspicuous by their near absence from the host of substrates that has been used in more than three decades of the MBH chemistry.[15–17] As for biological properties, besides the ones discussed above, although the anticancer properties of many nitro compounds have been investigated,[18] such properties of conjugated nitroalkenes per se have not received much attention.[19] Furthermore, although several compounds, both natural as well as synthetic, have been found to interfere with the microtubules in recent years, the possible interaction of nitroalkenes with microtubules has not received much attention.[20]

The key role of microtubules in cell division and mitosis makes them important chemotherapeutic drug targets for several diseases including cancer, parasitic diseases, and fungal diseases.[21] For example, several clinically successful drugs including paclitaxel, vinblastine, and estramustine target microtubules for their anticancer effects.[22] Microtubule targeting agents are broadly classified into two groups. One group of agents including vinblastine, colchicine, cryptophycin-52, and estramustine depolymerizes microtubules and the other group of compounds including paclitaxel, epothilones, and discodermolide increases microtubule polymerization.[23] Recent evidence strongly suggests that both stabilizing and destabilizing class of antimicrotubule agents inhibit cell proliferation by suppressing microtubule dynamics at their lower effective drug concentrations. The clinical success of microtubule targeted drugs prompted us to search for new agents that inhibit cell proliferation by targeting microtubules/tubulin.

Our preliminary results on the MBH reaction of nitroalkenes with formaldehyde have been published recently.[16] Under a program directed toward the synthesis and discovery of new anticancer agents, we report here the details of the synthesis of the α-hydroxymethylated nitroalkenes and the possible mechanism of their antiproliferative activity. We found that the tested conjugated nitroalkenes **1** and their hydroxymethylated derivatives **3** inhibited HeLa cell proliferation in the low micromolar concentrations with an apparent effect on cellular microtubules. They depolymerized cellular microtubules and inhibited tubulin polymerization in vitro. The results indicate that the tested nitroalkenes exert antiproliferative activity at least in part by depolymerizing microtubules through binding to tubulin. The antiproliferative activity of these agents is comparable to the potency of several tubulin-targeted antitumor agents including estramustine,[24–26] 2-methoxy estradiol,[27] sulfonamides,[28] and noscapine[29] indicating that some of the nitroalkenes may have potential to develop as anticancer drugs.

2. Results and discussion

2.1. Chemistry

We envisioned that the MBH adducts of nitroalkenes, if capable of binding to microtubules/tubulin, might possess enormous potential as drug candidates in the treatment of cancer. This is primarily because of the expected simplicity and efficiency associated with the synthesis of such molecules possessing functional groups as dense and diverse as a double bond, a nitro group, a hydroxyalkyl group, and an aryl group. Possible bioactivity of such small multifunctional molecules arising from hitherto unexplored reactivity of conjugated nitroalkenes as MBH substrates[16,20] motivated us to pursue their synthesis and biological evaluation.

All the nitroalkenes **1a–k** were prepared in the laboratory by the standard nitroaldol (Henry) reaction.[30] Attempted MBH type reaction of nitroalkene **1a** with formaldehyde **2** (38% aq, excess) as the electrophile in the presence of a variety of amine based catalysts such as DABCO, DBU, DMAP, Et_3N, and pyridine, and phosphine based catalysts, for example, $(n\text{-}Bu)_3P$, provided no satisfactory results.[13,14] Later, imidazole[31] emerged as the catalyst of choice and provided the desired MBH product **3a** in 40% yield. Complete conversion of the starting nitroalkene **1a** and improvement in the yield (48%), though marginal, was observed when stoichiometric amounts of imidazole were used (Table 1, entry 1a). Under these conditions, other nitroalkenes **1b–k** provided the desired MBH adducts **3b–k** in moderate yield (Fig. 1 and Table 1, entries 2a–11a). Subsequently, additives such as proline,[32] *o*-aminophenol, and anthranilic acid were screened for their co-catalytic activity. However, appreciable improvement in the yield (71%) was observed only when anthranilic acid was used as the co-catalyst (Table 1, entry 1b). THF was found to be superior to solvents such as DMF, MeOH, CH_3CN, and 1,4-dioxan. Finally, under the optimized conditions, that is, in the presence of imidazole (100 mol %) and anthranilic acid (10 mol %) in THF at room temperature, other nitroalkenes **1b–k** also reacted well with formaldehyde **2** and provided the hydroxymethylated products **3b–k** in satisfactory yields (Table 1, entries 2b–11b).

The geometry of the double bond in MBH adducts **3a–k** was determined by analysis of 2D-NOESY spectrum of a representative example **3a**. The methylene protons in **3a** exhibit strong positive NOE with all the furyl protons indicating *E* geometry for the double bond. However, in view of the methylene protons having strong positive NOE interaction with the olefinic proton as well and in view of any Z isomer being unavailable for comparison, further unambiguous confirmation of the structure was sought by X-ray crystallography. Thus, analysis of the MBH adduct **3b**, which provided suitable crystals, by X-ray crystallography unambiguously established the *E* geometry of the double bond.[33] Therefore, by analogy, *E* stereochemistry was assigned to all other MBH adducts, that is, **3a** and **3c–k**.

Table 1. The Morita–Baylis–Hillman reaction of nitroalkenes **1a–k** with formaldehyde **2**[a] in presence of 100 mol % (1 equiv) of imidazole and 10 mol % of anthranilic acid in THF at room temperature

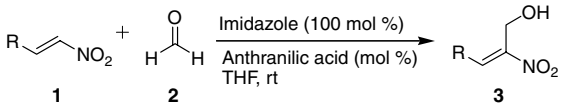

Entry	1	R	No additive (a)		AA[b] (10 mol %) (b)	
			Time (h)	% yield[c]	Time (h)	% yield[c]
1	**1a**	2-Furyl	20	48	24	71
2	**1b**	2-Thienyl	15	46	15	56
3	**1c**	3-Furyl	30	32	30	40
4	**1d**	3-Thienyl	30	29	30	35
5	**1e**	4-MeO-Ph	20	46	15	50
6	**1f**	2-NO_2-Ph	15	57	16	55
7	**1g**	3,4-$(MeO)_2$-Ph	36	44	36	46
8	**1h**	3-MeO-4-OH-Ph	24	56	24	60
9	**1i**	3,4-(–OCH_2O–)Ph	48	42	120	63
10	**1j**	4-F-Ph	30	24	30	25
11	**1k**	Ph	148	19	24	50

[a] 38% aqueous formaldehyde.
[b] Anthranilic acid.
[c] Isolated yield of **3** after purification by silica gel column chromatography.

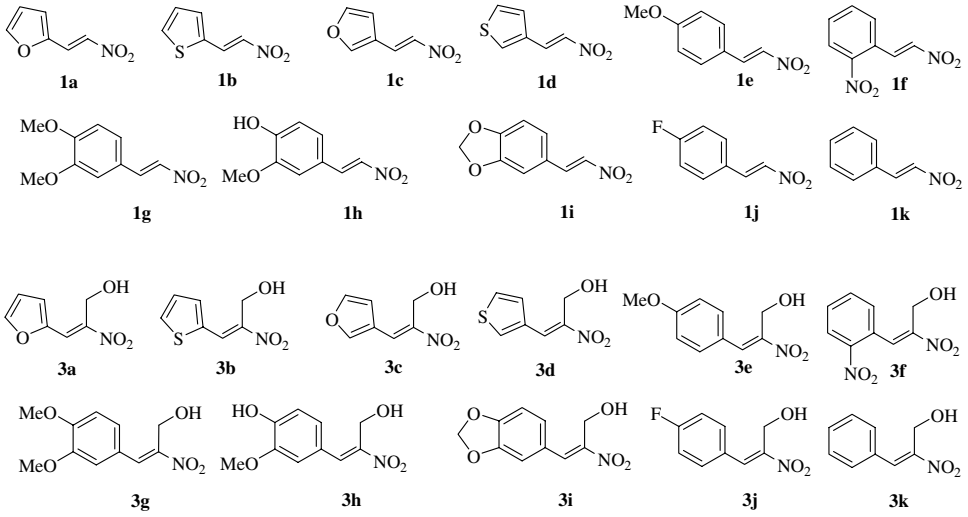

Figure 1. The nitroalkenes **1a–k** and corresponding hydroxymethylated products **3a–k**.

Insofar as the imidazole mediated MBH reaction of nitroalkenes **1** with formaldehyde is concerned (vide supra), the co-catalytic behavior of anthranilic acid is much in evidence from the substantial improvement in the yield of **3** in majority of the cases when the imidazole mediated reactions were carried out in the presence of 10 mol % of anthranilic acid as additive. This was further confirmed by carrying out the reaction of **1a** with formaldehyde **2** in the presence of aniline and benzoic acid as additives. The yields were only 41% and 44%, respectively, in these reactions. Therefore, anthranilic acid appears to serve, besides as a buffer that prevents (minimizes) nucleophile promoted oligomerization (polymerization) of the nitroalkene substrates, as a bifunctional catalyst in this reaction via (a) formation of hydrogen bonding between the carboxylic acid group of anthranilic acid and the nitro group of the substrate; (b) imine/iminium formation by the amino group of anthranilic acid and the carbonyl group of the electrophile. Such templating effect has been attributed to the catalytic activity of other organocatalysts, the classic example being proline.[32,34]

2.2. Biology

2.2.1. Inhibition of HeLa cell proliferation by nitroalkene derivatives. In order to test whether parent nitroalkenes **1** and their MBH adducts **3** could inhibit HeLa cell proliferation, cells were treated with different concentrations of the compounds. Cell viability was measured by the standard sulforhodamine B assay.[35] While most of the compounds inhibited HeLa cell proliferation (Table 2), three compounds, namely **1h**, **3h**, and **3j**, did not inhibit cell proliferation. Further detailed studies

Table 2. The IC_{50} values of nitroalkenes **1** and their MBH adducts **3** for HeLa cell proliferation

Entry	R	(a)		(b)	
		1	IC_{50} (μM)	**3**	IC_{50} (μM)
1	2-Furyl	**1a**	38 ± 3	**3a**	22 ± 4
2	2-Thienyl	**1b**	18 ± 2	**3b**	2 ± 1
3	3-Furyl	**1c**	2 ± 1	**3c**	5 ± 3
4	3-Thienyl	**1d**	3 ± 2	**3d**	5 ± 2
5	4-MeO-Ph	**1e**	17 ± 4	**3e**	2 ± 1
6	2-NO_2-Ph	**1f**	25 ± 3	**3f**	>50
7	3,4-$(MeO)_2$-Ph	**1g**	12 ± 1	**3g**	3 ± 1
8	3-MeO-4-OH-Ph	**1h**	[a]	**3h**	[a]
9	3,4-(–OCH_2O–)Ph	**1i**	18 ± 1	**3i**	38 ± 3
10	4-F-Ph	**1j**	4 ± 3	**3j**	[a]
11	Ph	**1k**	5 ± 1	**3k**	40 ± 2

[a] No inhibition. Data are means ± SD of five independent experiments.

were carried out with four potent representative compounds **1c**, **3b**, **3e**, and **3g**, which inhibited HeLa cell proliferation in a concentration dependent manner with half-maximal inhibitory concentration of proliferation in the range 2–3 μM (Table 2, entries 3a, 2b, 5b, and 7b). The antiproliferative effects of **1c**, **3b**, **3e**, and **3g** are comparable to those of the known tubulin interacting agents such as noscapine,[29] estramustine,[24–26] methoxyestradiol,[27] and griseofulvin[36] which are active in micromolar concentrations.

2.2.2. Structure–activity relationship. On the basis of the half-maximal inhibitory concentrations (IC_{50}) for HeLa cell proliferation determined for nitroalkenes **1a–k** and for the corresponding MBH adducts **3a–k** (Table 2), following inferences can be drawn. Among the four heteroaromatic nitroalkenes **1a–d** (entries 1a–4a), two, that is **1c** and **1d**, have low IC_{50} values (entries 3a and 4a). These agents have the nitroethylene moiety at position 3 of the heteroaromatic ring as opposed to **1a** and **1b** whose heteroaromatic rings are substituted by nitroethylene moiety at position 2. Among the seven aromatic nitroalkenes **1e–1k** screened (Table 2, entries 5a–11a), only **1j** and **1k** have low IC_{50} values (entries 10a and 11a). The result indicated that the presence of substituents such as NO_2, OMe, OH, and –OCH_2O– on the aromatic ring of the parent nitroalkene **1k** is not favorable. Comparison of the IC_{50} values of the MBH adducts **3** with those of the parent nitroalkenes **1** shows that, in majority of the cases, introduction of the hydroxymethyl moiety in **1** by the MBH reaction led to substantially low or at least comparable IC_{50} values (Table 2, entries 1–11). The exceptions are entries 6, 9, 10, and 11 (Table 2). Therefore, the MBH reaction of nitroalkenes turned out to be a useful strategy in our search for novel small multifunctional molecules that interact with the microtubules. Another comparison between the IC_{50} values of the MBH adducts of aromatic nitroalkenes **3e–k** (Table 2, entries 5b–11b) with those of heteroaromatic ones **3a–d** (entries 1b–4b) shows that, with the exception of **3e** and **3g**, the former have IC_{50} values higher than the latter. Interestingly enough, both **3e** and **3g** which have unusually low IC_{50} values possess OMe group(s) on the aromatic ring. Further comparison of **3g**, and **3h** shows that OMe group at the para position plays a significant role in lowering the IC_{50} value because its replacement with a hydroxy group results in complete loss of activity (Table 2, entries 7b and 8b).

2.2.3. Effect of 1c, 3b, 3e, and 3g on cellular microtubules. Immunofluorescence microscopic analysis was carried out to analyze the effects of MBH adducts **3b**, **3e**, **3g**, and a parent nitroalkene **1c** on interphase and spindle microtubules, and chromosome organization (Fig. 2). These agents were used at concentrations either equal to their IC_{50} values or two to three times higher than their IC_{50} values. Untreated cells displayed a regular network of interphase microtubules (Fig. 2A) and a normal mitotic spindle with proper chromosome alignment in the mitotic cells (Fig. 2I). Cells treated with 1 and 2 μM of **3e** showed normal interphase microtubules (Fig. 2B). The interphase microtubule organization of HeLa cells was also not perturbed in the presence of low concentrations (1 and 2 μM) of compounds **3b**, **3g**, and **1c** (data not shown). Higher concentrations (5 and 10 μM) of these compounds caused significant depolymerization of interphase microtubules (Fig. 2C, D, E, F, and H). In these cells, some of the microtubules appeared to be bundled. In cells treated with 10 μM of **3g**, interphase microtubules were strongly depolymerized and tubulin aggregates were observed in these cells (Fig. 2G).

Cells treated with 2 μM of **3b**, **3e**, **3g**, and **1c** showed abnormality in the spindle microtubules as well as in the chromosome alignment. In these cells mitotic spindles were either multipolar (Fig. 2J, L, and N) or abnormal bipolar (Fig. 2O) and chromosomes were unable to congress at the metaphase plate. Abnormal bipolar spindles contained chromosomes that were located near the spindle poles. A major population of the mitotic cells was found to have multipolar spindles. The effect was seen even at 1 μM in the case of cells treated with **3b** and **3g** (Fig. 2K and M). At 5 and 10 μM of **3b**, **3e**, and **3g**, mitotic cells were not readily detectable, which might be due to the strong depolymerizing effect of these agents on the interphase microtubules that the cells were unable to progress to the mitosis. However, mitotic cells were found at 5 and 10 μM of **1c**. In the presence of 10 μM of **1c**, unipolar spindles were observed (Fig. 2Q). Thus, **3b**, **3e**, **3g**, and **1c** depolymerized cellular microtubules and perturbed chromosome organization, which might be responsible for the antiproliferative effect of these agents on HeLa cells.

2.2.4. Effect of 3b, 3e, 3g, and 1c on tubulin polymerization in vitro. Since compounds **3b**, **3e**, **3g**, and **1c** depolymerized cellular microtubules, we examined their effects on the assembly of microtubules in vitro. The effects of **3b**, **3e**, **3g**, and **1c** on the polymerization of purified tubulin in 1 M glutamate buffer, pH 6.8, are shown in Figure 3.[37,38] Ten micromolars of **3b**, **3e**, **3g**, and **1c** decreased the light scattering signal for microtubule assembly by 32%, 37%, 33%, and 35%, respectively, suggesting that the four MBH adducts inhibited microtubule assembly.

Further, the effects of **3b**, **3e**, **3g**, and **1c** on microtubule polymerization were analyzed by transmission electron microscopy (Fig. 4). Electron microscopic analysis showed that 10 μM of compounds **3b**, **3e**, **3g**, and **1c**

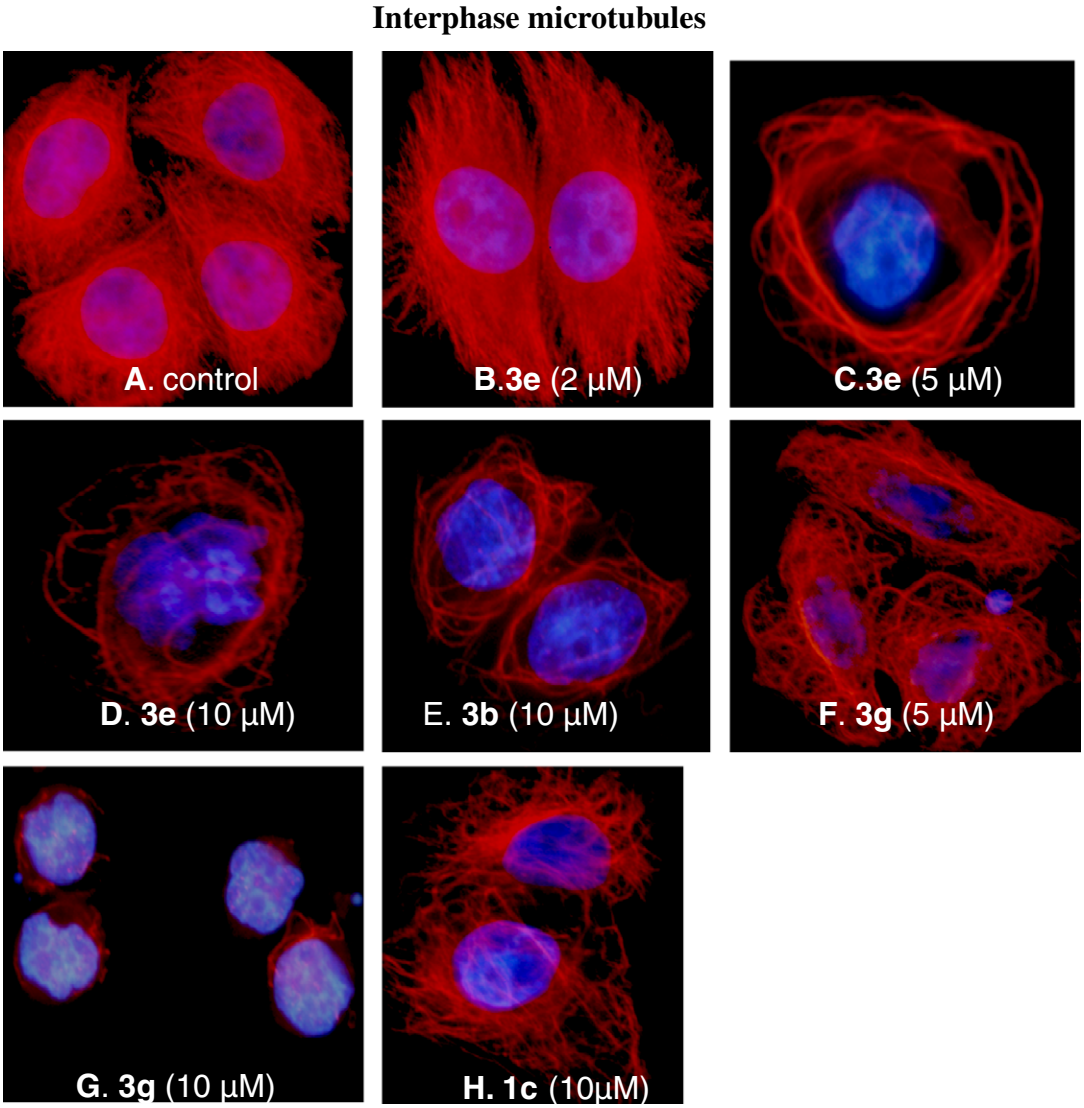

Figure 2. Effect of compounds **3e**, **3b**, **3g**, and **1c** on interphase and spindle microtubules. HeLa cells were grown in the absence and presence of different concentrations of **3e**, **3b**, **3g**, and **1c** for 24 h. (A) control interphase cells with fine network of microtubules; (B) 2 μM of **3e** had no effect on interphase microtubules; (C, D, E, F, and H) 5 μM **3e**, 10 μM **3e**, 10 μM **3b**, 5 μM **3g**, and 10 μM **1c**, respectively, induced interphase microtubule depolymerization; (G) 10 μM of **3g** caused significant depolymerization of interphase microtubules, tubulin aggregates are also observed; (I) control cells showed normal mitotic spindle with proper chromosome alignment at the metaphase plate; (J, K, L, M, and N) 2 μM of **3e**, 1 μM of **3b**, 2 μM of **3b**, 1 μM of **3g**, and 2 μM of **3g**, respectively, induced multipolar spindle formation. (O and P) cells treated with 2 μM of **1c** and 5 μM of **1c** had abnormal bipolar spindles with uncongressed chromosomes. (Q) cells treated with 10 μM of **1c** showed unipolar spindles.

inhibited polymerization of tubulin into microtubules (Fig. 4B, D, F, and H). The number of tubulin polymers was significantly reduced and small aggregates of tubulin were also found at this concentration. Twenty-five micromolars of **3b**, **3e**, **3g**, and **1c** caused extensive aggregation of tubulin dimers (Fig. 4C, E, G, and I). Binding of these MBH adducts to tubulin may induce a conformational change in the tubulin thereby inhibiting its assembly to microtubules.

2.2.5. Binding of 3b, 3e, 3g, and 1c to tubulin. Changes in the intrinsic tryptophan fluorescence of tubulin upon ligand binding are widely used to determine the binding affinity of the ligands to tubulin.[36] Tubulin (1 μM) was incubated with a range of concentrations of **3b**, **3e**, **3g**, and **1c** for 30 min at 25 °C. Compound **3e** reduced the intrinsic tryptophan fluorescence of tubulin in a concentration dependent manner indicating that the agent induced conformational change in tubulin (Fig. 5A). Similarly, compounds **3b**, **3g**, and **1c** also reduced the intrinsic tryptophan fluorescence of tubulin in a concentration dependent manner (data not shown). A double reciprocal plot of the binding of **3e** with tubulin is shown (Fig. 5B). Using similar double reciprocal plots, the dissociation constant of nitroalkenes to tubulin interaction was determined to be 3 ± 1, 11 ± 4, 7 ± 1, and 5 ± 1 μM for **3b**, **3e**, **3g**, and **1c**, respectively. Data are mean ± SD of five independent experiments.

2.2.6. Inhibition of Tubulin-ANS fluorescence by 3b, 3e, 3g, and 1c. The non-covalent fluorescent probe 1-anilinonaphthalene-8-sulfonic acid (ANS) is widely used to analyze hydrophobic surface rearrangements of tubulin.[35,37,39–42] The strong ANS-tubulin fluorescence

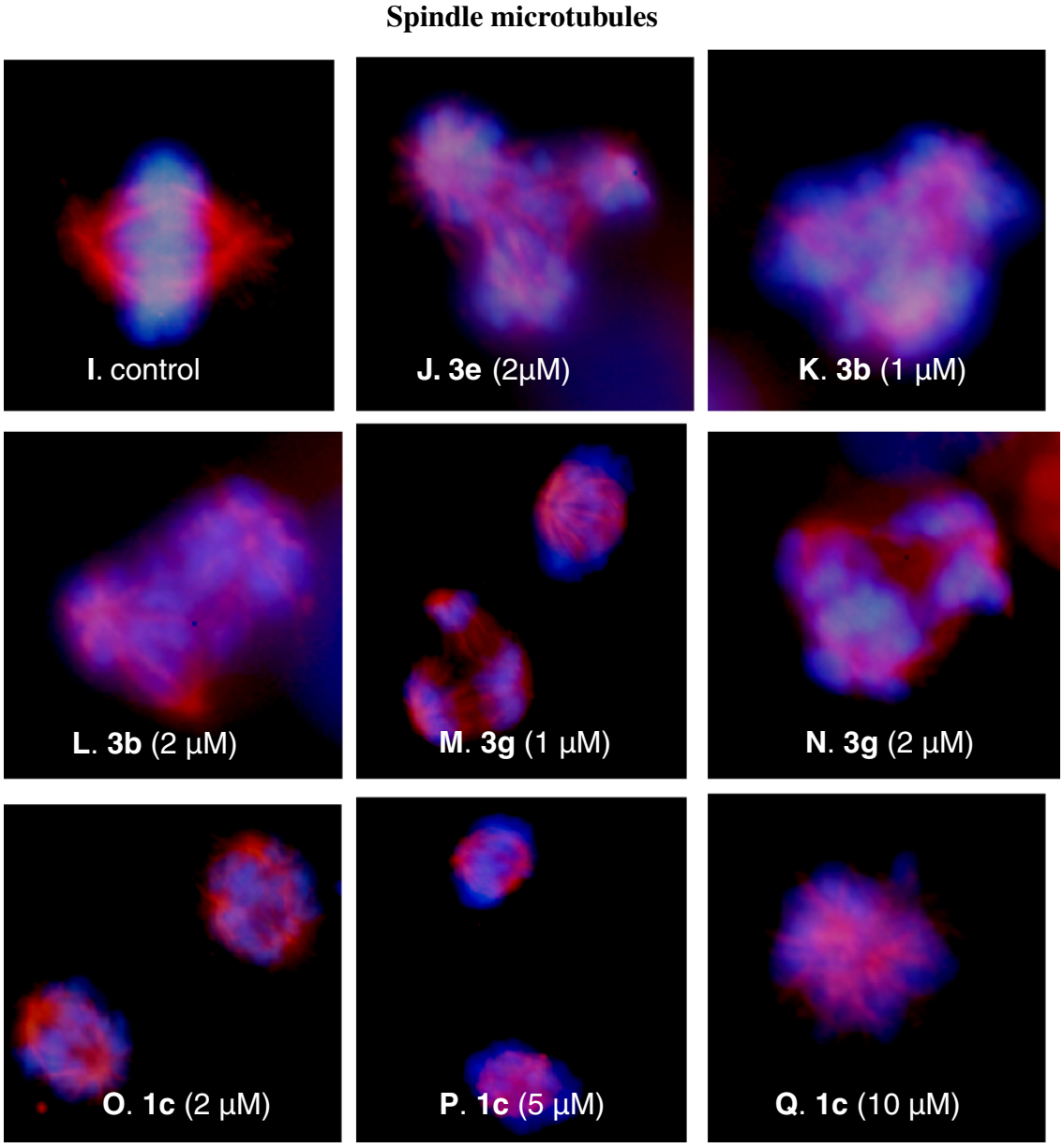

Figure 2. *(continued)*

was used to study the interaction of **3b**, **3e**, **3g**, and **1c** with tubulin. ANS (40 μM) was added to the preformed tubulin-**3a/3b/3g/1c** complex, and the effects of these compounds on tubulin-ANS fluorescence were monitored. The MBH adducts **3a**, **3b**, **3g**, and **1c** reduced the fluorescence intensity of tubulin-ANS complex by 30–40% (Fig. 6). The reduction in the fluorescence of tubulin-ANS complex upon binding to **3b**, **3e**, **3g** or **1c** may be due to conformational change induced in tubulin by MBH adducts or inhibition of ANS binding to tubulin by **3b**, **3e**, **3g**, and **1c**. A modest increase in tubulin-ANS fluorescence was observed at higher concentrations (>25 μM) of **3a**, **3b**, **3g**, and **1c**, which might be due to aggregation of the protein.

2.2.7. Characterization of the binding site of 3b, 3e, 3g, and 1c in tubulin. Microtubule interacting agents are known to bind to diverse sites on tubulin and several of these drugs induce conformational changes in tubulin upon binding to the protein. Using fluorescent analogue of vinblastine (BODIPY FL-vinblastine), we first examined whether **3b**, **3e**, **3g**, and **1c** competed with vinblastine for its binding to tubulin (Fig. 7).[35,43] Compounds **3b**, **3e**, **3g**, and **1c** increased the fluorescence of fluorescent vinblastine–tubulin complex, suggesting that it does not bind to the vinblastine binding site on tubulin. The increase in fluorescence of the tubulin–fluorescent vinblastine complex in the presence of **3b**, **3e**, **3g**, and **1c** may be due to the stabilization of vinblastine binding site on tubulin by these agents.[44,45]

Nitroalkenes (**3e**, **3b**, **3g**, and **1c**) reduced tubulin-ANS fluorescence in a concentration dependent manner (Fig. 6); therefore, we also used ANS fluorescence as a probe to determine whether **3e**, **3b**, **3g**, and **1c** bind at the vinblastine site on tubulin. ANS binds at a site that

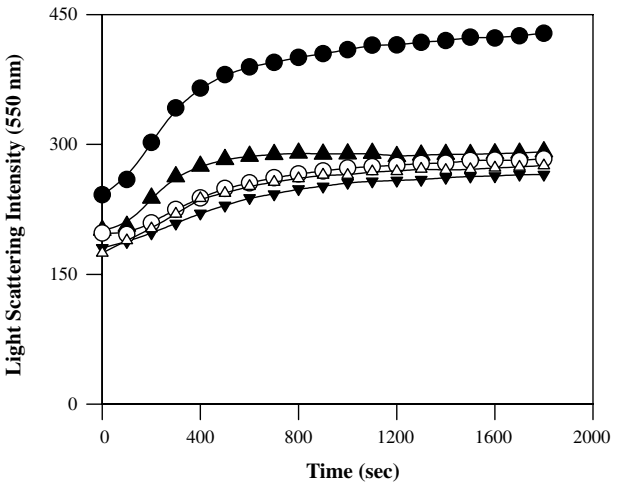

Figure 3. Inhibition of microtubule polymerization in the absence (●) and presence of 10 μM each of **3b** (▼), **3e** (▲), **3g** (○) and **1c** (△). Tubulin (10 μM) was polymerized in the absence and presence of 10 μM of **3b**, **3e**, **3g**, and **1c** and the change in the light scattering intensity at 550 nm was monitored. The percent inhibition of polymerization was calculated by considering the light scattering intensity of control sample as 100% after 30 min of assembly.

is different from the vinblastine binding site on tubulin.[39] First, tubulin–vinblastine complex was formed by incubating tubulin (3 μM) with 120 μM vinblastine on ice for 5 min. Then, ANS (100 μM) was added to the tubulin–vinblastine complex and further incubated for an additional 10 min at 25 °C. Incubation of ANS-tubulin–vinblastine complex with varying concentrations of **3e**, **3b**, **3g**, and **1c** decreased the fluorescence of ANS-tubulin–vinblastine complex in a concentration dependent manner (data not shown). The decrease in tubulin-ANS fluorescence with increasing concentrations of **3e**, **3b**, **3g**, and **1c** was found to be similar in the absence and presence of 120 μM vinblastine suggesting that the nitroalkenes **3e**, **3b**, **3g**, and **1c** and vinblastine do not share the same binding site on tubulin.

Colchicine has strong fluorescence when it binds to tubulin.[46] We used the fluorescence of tubulin–colchicine complex to determine whether **3b**, **3e**, **3g**, and **1c** and colchicine shared the same binding site in tubulin. We found that preincubation of tubulin with different concentrations of **3b**, **3e**, **3g**, and **1c** did not affect the fluorescence of colchicine–tubulin complex suggesting

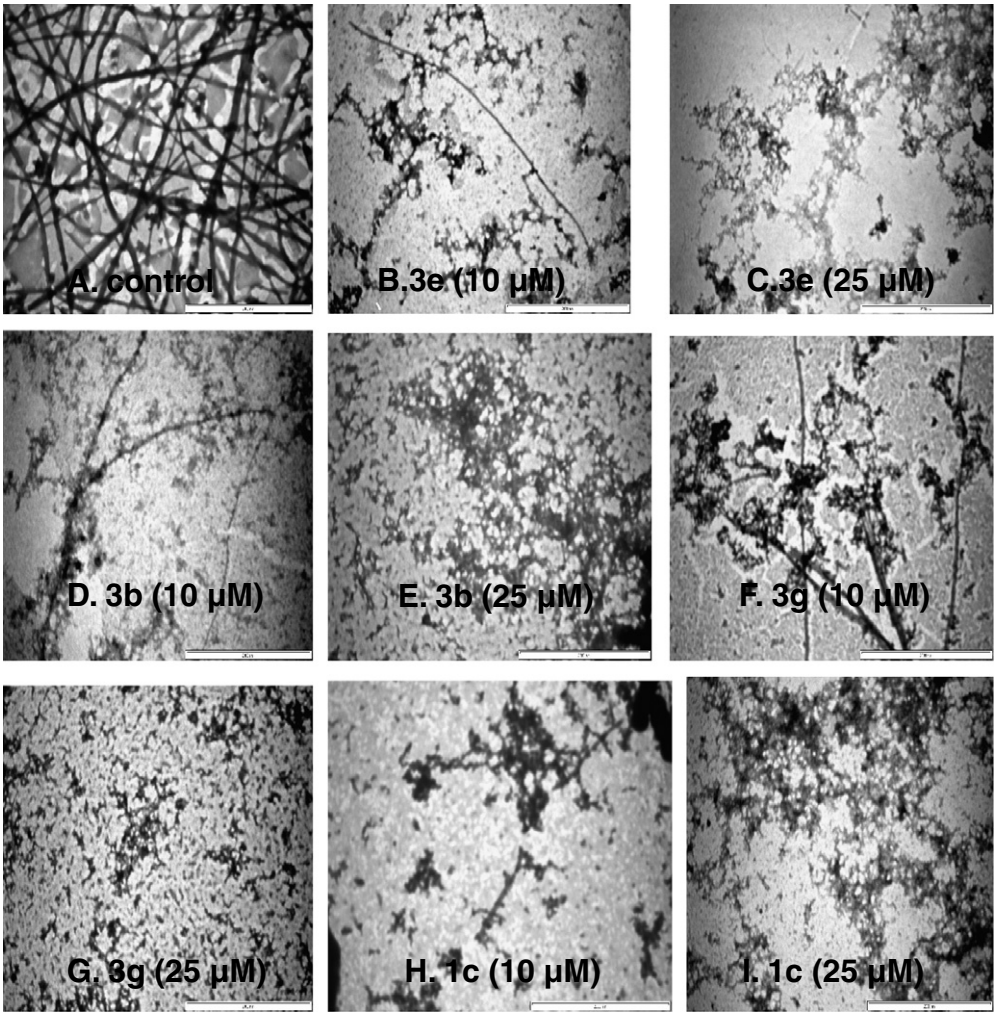

Figure 4. Electron microscopic visualization of tubulin polymers in the absence (A) and presence of 10 and 25 μM each of **3e**, **3b**, **3g**, and **1c**. These compounds inhibited tubulin polymerization at 10 μM (B, D, F, and H) and at 25 μM induced tubulin aggregation (C, E, G, and I). Images were taken at 16500× magnification. Scale bar represents 1000 nm.

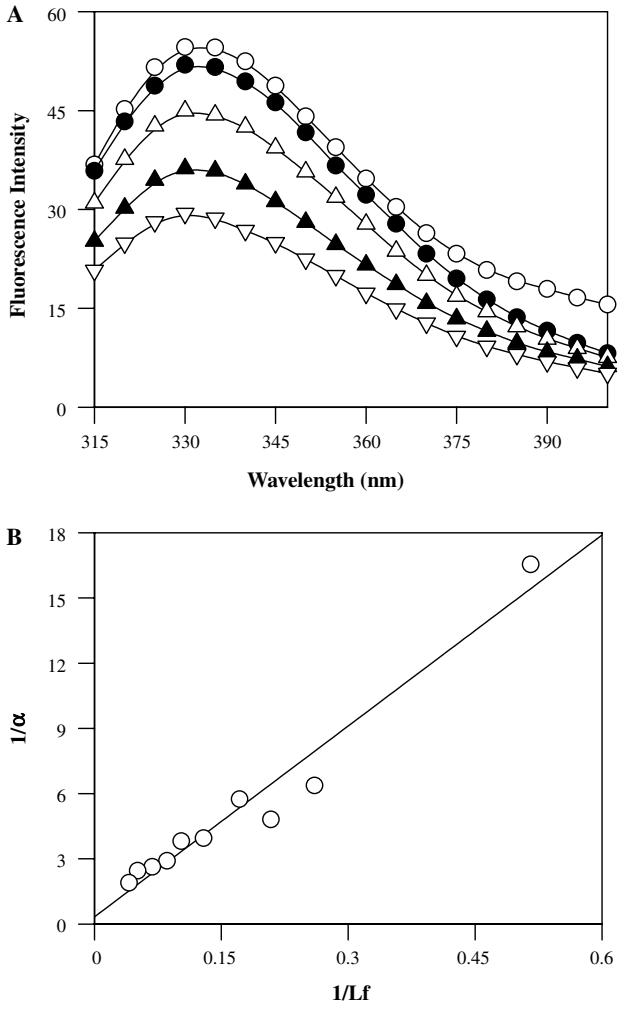

Figure 5. (A) Effect of **3e** on the intrinsic tryptophan fluorescence of tubulin. Tubulin (1 μM) was incubated in the absence (○) and presence of varying concentrations (2 (●), 5 (△), 15 (▲), and 25 (▽) μM) of **3e** in assembly buffer for 30 min at 25 °C. Fluorescence spectra were taken using 295 nm as an excitation wavelength. (B) Double reciprocal plot of binding of MBH adduct **3e** to tubulin.

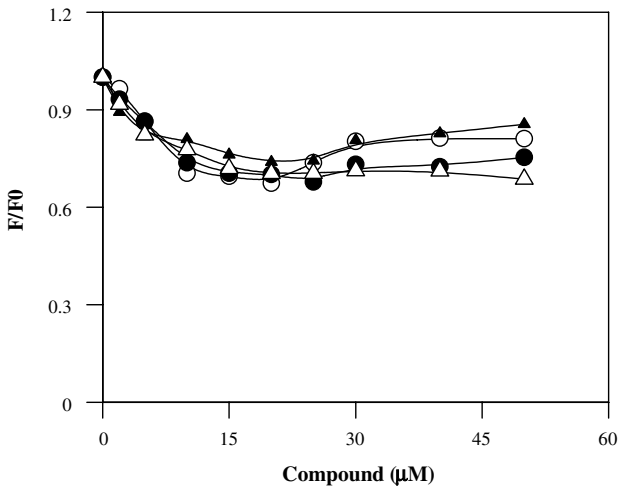

Figure 6. Reduction of tubulin-ANS complex fluorescence by varying concentrations of **3e** (○), **3b** (●), **3g** (▲), and **1c** (△).

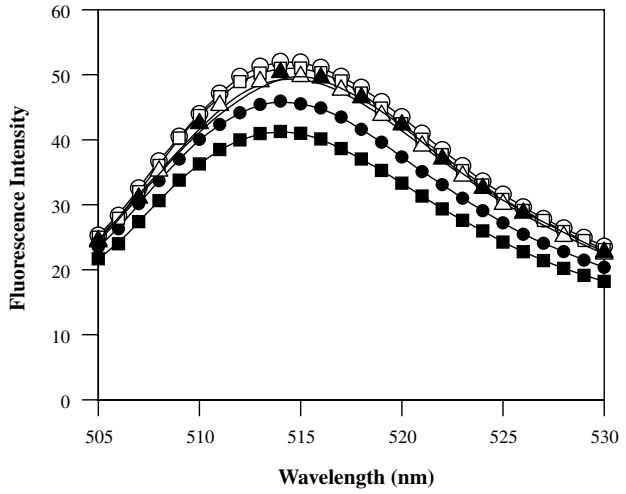

Figure 7. Effects of **3e**, **3b**, **3g**, and **1c** on the fluorescence of BODIPY FL-vinblastine–tubulin complex. Tubulin (3 μM) was incubated in the absence and presence of 25 μM each of **3e**, **3b**, **3g**, and **1c** at 37 °C for 45 min. Then, 2 μM fluorescent vinblastine was added to all the samples. Fluorescence spectra were collected using an excitation wavelength of 490 nm. Control (●), 100 μM unlabelled vinblastine (■), 25 μM each of **3e** (△), **3b** (○) **3g** (▲), and **1c** (□).

that **3b**, **3e**, **3g**, and **1c** did not inhibit colchicine binding to tubulin (data not shown).

We also determined the effects of **3b**, **3e**, **3g**, and **1c** on the kinetics of colchicine binding to tubulin. No reduction in the rate of colchicine binding to tubulin was observed in the presence of the tested nitroalkenes suggesting that these agents did not bind tubulin at the colchicine site (Fig. 8). The increase in the fluorescence of the tubulin–colchicine complex in the presence of **3b**, **3e**, **3g**, and **1c** may be due to the stabilization of colchicine binding site on tubulin by these agents. Taken together, the results suggest that **3b**, **3e**, **3g**, and **1c** do

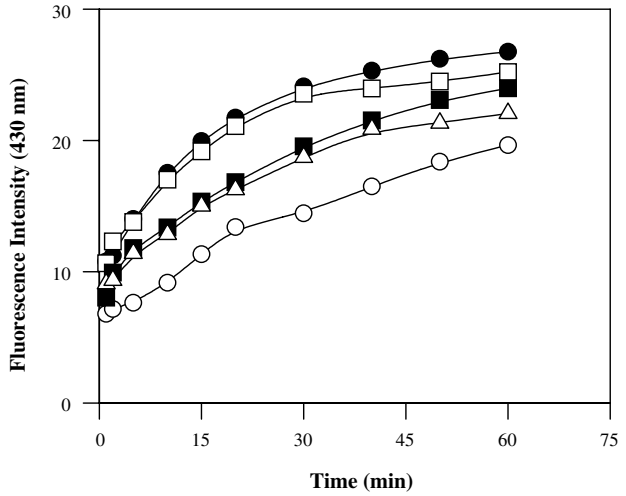

Figure 8. Kinetics of colchicine–tubulin binding in the absence (○) and in the presence of 25 μM each of **3b** (□), **3e** (●), **3g** (■), and **1c** (△). Tubulin was preincubated with 25 μM of **3b**, **3e**, **3g**, and **1c** and after adding 10 μM colchicine to the reaction mixtures, the fluorescence intensity was monitored over time. Excitation and emission wavelengths were 360 and 430 nm, respectively.

not bind to the vinblastine or colchicine binding sites on tubulin.

Compounds **3b**, **3e**, **3g**, and **1c** depolymerized cellular microtubules and inhibited tubulin polymerization by binding to tubulin indicating that the antiproliferative effect of nitroalkenes might be partly due to depolymerization of cellular microtubules. However, the possibility of other cellular targets for the tested nitroalkenes cannot be ruled out. Further, while most of the clinically used antimicrotubule agents are large molecules with complex structures, conjugated nitroalkenes **1** and their hydroxymethylated derivatives **3** tested here are small, simple, but multifunctional molecules that can be easily synthesized. This study might help develop more potent analogues, which will be useful for the treatment of tumor.

3. Conclusions

Conjugated nitroalkenes are amenable for the Morita–Baylis–Hillman (MBH) type reaction under suitable experimental conditions. The multifunctional MBH adducts inhibit proliferation of cancer cells apparently by depolymerizing cellular microtubules. The microtubules were found to undergo depolymerization at lower concentrations and aggregation at higher concentrations of the MBH adducts. While the compounds studied bind to tubulin and induce conformational changes, they did not bind to the well-known binding sites of colchicine and vinblastine. Our results suggest that even small, simple, and easily accessible multifunctional molecules such as the ones reported in this paper could be useful for cancer therapy.

4. Experimental

4.1. General

The melting points are uncorrected. IR spectra were recorded on an Impact 400/Nicolet FT spectrometer. NMR spectra (^{1}H and ^{13}C) were recorded on an AMX-400 or VXR-300S spectrometer with TMS as the internal standard. High-resolution mass spectra (DCI in CH_4 or *i*-butane) were recorded at 60–70 eV on a VG-Fisons 'Autospec' spectrometer. X-ray data were collected on a NONIUS MACH3 diffractometer. GTP, Pipes, vinblastine, and colchicine were obtained from Sigma (St. Louis, MO). Fluorescent vinblastine (BODIPY FL-vinblastine) was obtained from Molecular Probes (Eugene, OR) and phosphocellulose (P11) was from Whatman (Maidstone, England). Monoclonal anti α-tubulin antibody and 4,6-diamidino-2-phenylindole (DAPI) were obtained from Sigma (St. Louis, MO) and Alexa 568 conjugated sheep anti-mouse IgG antibody was obtained from Molecular probes. All the other reagents were of analytical grade.

4.2. Chemistry

4.2.1. General procedure for the MBH reaction of nitroalkenes 1 with formaldehyde 2. To a stirred solution of nitroalkenes **1** (1 mmol) in THF (2 ml) at room temperature was added imidazole (68 mg, 1 equiv) followed by anthranilic acid (14 mg, 10 mol %). Aqueous formaldehyde **2** (38%, 2 ml, excess) was then added and the reaction mixture was stirred at room temperature for the period specified in Table 1. After the completion of the reaction (confirmed by TLC analysis), the reaction mixture was acidified with 5 N HCl (5 ml) and the aqueous layer was extracted with ethylacetate (3×10 ml). The combined organic layers were washed with brine (10 ml), dried over anhydrous Na_2SO_4, and concentrated in vacuo. The residue was purified by silica gel column chromatography by eluting with EtOAc/pet. ether (0–25%, gradient elution) to afford pure **3**.

4.2.1.1. (*2E*)-3-(2-Furyl)-2-nitroprop-2-en-1-ol (3a). Yellow crystalline solid; yield: 71%; mp 87–89 °C (CH_2Cl_2-pet. ether 1:3). IR (KBr) cm^{-1} 3434 (br s), 1651 (s), 1519 (s), 1315 (s), 1025 (s), 742 (s). ^{1}H NMR ($CDCl_3$) δ 2.48 (br s, 1H), 5.04 (s, 2H), 6.62 (dd, J = 3.3 Hz, J = 1.8 Hz, 1H), 6.99 (d, J = 3.3 Hz, 1H), 7.70 (d, J = 1.8 Hz, 1H), 7.88 (s, 1H). ^{13}C NMR ($CDCl_3$) δ 56.7 (t), 113.3 (d), 122.1 (d), 122.7 (d), 145.7 (s), 146.9 (s), 147.6 (d); MS (DCI, CH_4) *m/e* (rel intensity) 169 (M^+, 100), 153 (38), 147 (36), 133 (11); HRMS (DCI, CH_4) Calcd for $C_7H_7NO_4$ (M^+, 100) 169.0375, found 169.0381.

4.2.1.2. (*2E*)-2-Nitro-3-(2-thienyl)prop-2-en-1-ol (3b). Yellow crystalline solid; yield: 56%; mp 104–105 °C (CH_2Cl_2-pet. ether 1:3). IR (KBr) cm^{-1} 3513 (br s), 3098 (m), 2954 (s), 1644 (s), 1512 (m), 1315 (s), 1025 (m), 736 (m). ^{1}H NMR ($CDCl_3$) δ 2.72 (br s, 1H), 4.83 (s, 2H), 7.12 (dd collapsed to t, J = 4.4 Hz, 1H), 7.47 (d, J = 3.7 Hz, 1H), 7.62 (d, J = 5.1 Hz, 1H), 8.20 (s, 1H). ^{13}C NMR ($CDCl_3$) δ 56.9 (t), 128.7 (d), 130.4 (d), 133.5 (d), 133.6 (s), 136.3 (d), 146.3 (s); MS (DCI, CH_4) *m/e* (rel intensity) 185 (M^+, 37), 169 (43), 168 (73), 138 (21), 122 (34), 112 (100), 110 (29), 109 (25), 97 (20); HRMS (DCI, CH_4) Calcd for $C_7H_7NO_3S$ (M^+, 37) 185.0147, found 185.0156.

4.2.1.3. (*2E*)-3-(3-Furyl)-2-nitroprop-2-en-1-ol (3c). Yellow crystalline solid; yield: 40%; mp 71–73 °C (CH_2Cl_2-pet. ether 1:3). IR (KBr) cm^{-1} 3351 (br s), 3140 (s), 2959 (s), 1648 (s), 1516 (s), 1315 (s), 1159 (s), 1020 (s), 860 (m). ^{1}H NMR ($CDCl_3$) δ 2.20 (br s, 1H), 4.77 (s, 2H), 6.75 (m, 1H), 7.57 (m, 1H), 7.91 (m, 1H), 8.04 (s, 1H). ^{13}C NMR ($CDCl_3$) δ 56.6 (t), 109.9 (d), 118.2 (s), 128.5 (d), 145.3 (d), 147.4 (d), 147.8 (s); MS (DCI, CH_4) *m/e* (rel intensity) 169 (M^+, 100), 152 (2), 146 (5), 143 (2); HRMS (DCI, CH_4) Calcd for $C_7H_7NO_4$ (M^+, 100) 169.0375, found 169.0322.

4.2.1.4. (*2E*)-2-Nitro-3-(3-thienyl)prop-2-en-1-ol (3d). Yellow crystalline solid; yield: 35%; mp 94–95 °C (CH_2Cl_2-pet. ether 1:3). IR (KBr) cm^{-1} 3303 (br, m), 3102 (m), 2956 (m), 1634 (s), 1509 (m), 1301 (s), 1260 (s), 1100 (s), 1013 (s), 875 (m). ^{1}H NMR ($CDCl_3$) δ 2.62 (br s, 1H), 4.78 (s, 2H), 7.37 (dd, J = 5.0, 0.9 Hz, 1H), 7.46 (dd, J = 5.0, 2.9 Hz, 1H), 7.82 (dd, J = 2.9, 0.9 Hz, 1H), 7.82 (s, 1H). ^{13}C NMR ($CDCl_3$) δ 56.6 (t), 127.5 (d), 128.3 (d), 131.5 (d), 131.7 (d), 132.5 (s), 147.9 (s); MS (DCI, CH_4) *m/e* (rel intensity) 185 (M^+,

100), 168 (31), 156 (14), 140 (27), 138 (19), 137 (20), 122 (65), 111 (73), 110 (61), 109 (90), 97 (28); HRMS (DCI, CH_4) Calcd for $C_7H_7NO_3S$ (M^+, 100) 185.0147, found 185.0141.

4.2.1.5. (*2E*)-3-(4-Methoxyphenyl)-2-nitroprop-2-en-1-ol (3e). Yellow crystalline solid; yield: 50%, mp 74–75 °C (CH_2Cl_2-pet. ether 1:3). IR (KBr) cm^{-1} 3441 (br s), 2960 (s), 1611 (s), 1519 (s), 1315 (m), 1269 (s), 1098 (s), 1032 (s), 808 (s). ^1H NMR ($CDCl_3$) δ 1.60 (br s, 1H), 3.88 (s, 3H), 4.73 (s, 2H), 7.0 (d, $J = 9.0$ Hz, 2 H), 7.56 (d, $J = 9.0$ Hz, 2H), 8.20 (s, 1H). ^{13}C NMR ($CDCl_3$) δ 55.5 (q), 56.8 (t), 114.7 (d), 123.6 (s), 132.6 (d), 138.0 (d), 147.4 (s), 162.1 (s); MS (DCI, CH_4) *m/e* (rel intensity) 209 (M^+, 100), 193 (21), 192 (16), 181 (14), 162 (38), 146 (65), 135 (30), 131 (30). HRMS (DCI, CH_4) Calcd for $C_{10}H_{11}NO_4$ (M^+, 100) 209.0688, found 209.0699.

4.2.1.6. (*2E*)-2-Nitro-3-(2-nitrophenyl)prop-2-en-1-ol (3f). Yellow oil; yield: 56%. IR (film) cm^{-1} 3459 (br s), 3105 (m), 2940 (m), 1539 (s), 1354 (s), 1038 (m), 749 (w). ^1H NMR ($CDCl_3$) δ 2.40 (br s, 1H), 4.52 (s, 2H), 7.65–7.83 (m, 3H), 8.30 (d, $J = 12$ Hz, 1H), 8.51 (s, 1H). ^{13}C NMR ($CDCl_3$) δ 56.5 (t), 125.5 (d), 127.6 (d), 131.2 (d), 131.6 (d), 134.5 (d), 134.8 (s), 147.4 (s), 149.8 (s); MS (DCI, CH_4) 225 (MH^+, 19), 208 (19), 207 (100), 162 (10), 160 (11), 135 (16), 132 (11), 120 (82), 92 (23); HRMS (DCI, CH_4) Calcd for $C_9H_8N_2O_5$ (MH^+, 19) 225.0511, found 225.0516.

4.2.1.7. (*2E*)-3-(3,4-Dimethoxyphenyl)-2-nitroprop-2-en-1-ol (3g). Yellow crystalline solid; yield: 46%; mp 97–99 °C (CH_2Cl_2-pet. ether 1:3). IR (KBr) cm^{-1} 3520 (br s), 2957 (m), 1626 (m), 1530 (s), 1274 (s), 1159 (m), 1038 (s), 814 (m). ^1H NMR ($CDCl_3$) δ 1.70 (br s, 1H), 3.93 (s, 3H), 3.95 (s, 3H), 4.74 (s, 2H), 6.96 (d, $J = 8.2$ Hz, 1H), 7.17 (dd, $J = 2.0$, 0.5 Hz, 1H), 7.25 (dd, $J = 8.2$, 0.5 Hz, 1H), 8.19 (s, 1H). ^{13}C NMR ($CDCl_3$) δ 56.1 (q), 56.2 (q), 57.1 (t), 111.4 (d), 113.0 (d), 124.1 (s), 124.9 (d), 138.4 (d), 147.7 (s), 149.4 (s), 151.9 (s); MS (DCI, CH_4) 239 (M^+, 100), 192 (28); HRMS (DCI, CH_4) Calcd for $C_{11}H_{13}NO_5$ (M^+, 100) 239.0794, found 239.0799.

4.2.1.8. (*2E*)-3-(4-Hydroxy-3-methoxyphenyl)-2-nitroprop-2-en-1-ol (3h). Yellow crystalline solid; yield: 60%; mp 92–94 °C (CH_2Cl_2-pet. ether 1:3). IR (KBr) cm^{-1} 3482 (br s), 2976 (m), 1645 (w), 1600 (m), 1517 (m), 1274 (s), 1089 (s), 1031 (s), 801 (s). ^1H NMR ($CDCl_3$) δ 1.62 (br s, 1H), 3.96 (s, 3H), 4.74 (s, 2H), 6.04 (br s, 1H), 7.01 (d, $J = 8.9$ Hz, 1H), 7.16–7.20 (m, 2H), 8.18 (s, 1H). ^{13}C NMR ($CDCl_3$) δ 56.1 (q), 57.0 (t), 112.5 (d), 115.2 (d), 123.5 (s), 125.5 (d), 138.5 (d), 146.9 (s), 147.4 (s), 148.8 (s); MS (DCI, CH_4) 225 (M^+, 100), 178 (35), 162 (20), 152 (9), 135 (14), 107 (8), 91 (13); HRMS Calcd for $C_{10}H_{11}NO_5$ (M^+,100) 225.0637, found 225.0639.

4.2.1.9. (*2E*)-3-(Benzo-[*d*][1,3]dioxol-5-yl)-2-nitroprop-2-en-1-ol (3i). Yellow crystalline solid; yield: 63%; mp 100–102 °C (CH_2Cl_2-pet. ether 1:3). IR (KBr) cm^{-1} 3450 (br s), 1632 (m), 1511 (m), 1332 (m), 1031 (w), 820 (w). ^1H NMR ($CDCl_3$) δ 4.64 (s, 2H), 5.99 (s, 2H), 6.83 (d, $J = 8.6$ Hz, 1H), 7.1 (m, 2H), 8.1 (s, 1H). ^{13}C NMR ($CDCl_3$) δ 56.94 (t), 102.12 (t), 109.23 (d), 109.98 (d), 125.34 (s), 126.7 (d), 138.1 (d), 148.0 (s), 148.8 (s), 150.6 (s); MS (DCI, CH_4) *m/e* (rel. intensity) 223 (M^+, 48), 183 (25), 150 (15), 149 (11), 147 (14); HRMS Calcd for $C_{10}H_9NO_5$ (M^+, 48) 223.0481, found 223.0480.

4.2.1.10. (*2E*)-3-(4-Fluorophenyl)-2-nitroprop-2-en-1-ol (3j). Yellow crystalline solid; yield: 25%; mp 52–54 °C (CH_2Cl_2-pet. ether 1:3). IR (KBr) cm^{-1} 3459 (br s), 2952 (m), 1655 (w), 1603 (m), 1516 (s), 1326 (s), 1235 (s), 1159 (w), 1020 (s), 843 (m). ^1H NMR ($CDCl_3$) δ 2.35 (br s, 1H), 4.68 (s, 2H), 7.18 (dd collapsed to t, $J = 8.6$ Hz, 2H), 7.60 (dd, $J = 8.9$, 5.2 Hz, 2H), 8.18 (s, 1H). ^{13}C NMR ($CDCl_3$) δ 56.6 (t), 116.5, 116.7 (dd), 127.6 (s), 132.6, 132.7 (dd), 136.8 (d), 149.3 (s), 163.1, 165.6 (sd); MS (DCI, CH_4) *m/e* (rel intensity) 197 (M^+, 21), 181 (45), 169 (100), 150 (21), 149 (52), 134 (75), 133 (38), 131 (43), 123 (28), 122 (45), 121 (49), 119 (67), 109 (23), 101 (50); HRMS calcd for $C_9H_8NO_3F$ (M^+, 21) 197.0488, found 197.0460.

4.2.1.11. (*2E*)-2-Nitro-3-(phenyl)prop-2-en-1-ol (3k). Yellow oil; yield: 50%; IR (film) cm^{-1} 3445 (br s), 2947 (m), 1653 (m), 1528 (s), 1338 (s), 1023 (s), 695 (m). ^1H NMR ($CDCl_3$) δ 2.96 (t, $J = 5.8$ Hz, 1H), 4.70 (d, $J = 5.8$ Hz, 2H), 7.46–7.58 (m, 5H), 8.20 (s, 1H). ^{13}C NMR ($CDCl_3$) δ 56.5 (t), 129.1 ($2 \times$ d), 130.1 ($2 \times$ d), 130.9 (d), 131.2 (s), 137.7 (d), 149.3 (s); MS (DCI, CH_4) *m/e* (rel intensity) 179 (M^+, 32), 162 (82), 116 (100), 115 (64), 103 (87), 91 (59); HRMS Calcd for $C_9H_9NO_3$ (M^+) 179.0582, found 179.0585.

4.3. Biology

4.3.1. Cell culture. HeLa cells were cultured in Eagle's minimal essential medium (MEM) supplemented with 10% fetal calf serum, 1.5 g/L sodium bicarbonate and 1% antibiotic–antimycotic solution containing streptomycin, amphotericin B, and penicillin. Cells were maintained at 37 °C in a humidified atmosphere of 5% carbon dioxide and 95% air. Cells were seeded at a density of 1×10^5 cells/ml on 96-well plates. For immunofluorescence studies, 0.6×10^5 cells/ml were grown as a monolayer on poly(L-lysine) coated coverslips. Compounds diluted in dimethylsulfoxide (DMSO) (0.1% final concentration) were added to the culture medium 24 h after seeding.

4.3.2. Cell proliferation assay. 1×10^5 cells/ml were seeded in each well in 96-well plates for 24 h and further incubated with different concentrations of compounds at 37 °C for 24 h. After 24 h, cell growth was stopped by the addition of 10% trichloroacetic acid and stained with 0.4% sulforhodamine B dissolved in 1% acetic acid. Unbound dye was removed by washing with 1% acetic acid and the protein content was determined by measuring absorbance at 560 nm in a Bio-Rad Model 680 microplate reader after extracting with 10 mM Tris base. IC_{50} is the drug concentration that inhibits the cell proliferation by 50% relative to the untreated control cells. Data are the average of five independent experiments.

4.3.3. Immunofluorescence microscopy. Cells (0.6×10^5 cells/ml) seeded on poly(L-lysine) coated coverslips were exposed to different concentrations (0, 1, 2, 5, and 10 μM) of **3b**, **3e**, **3g**, and **1c** for 20 h at 37 °C. Cells were fixed in 3.7% formaldehyde and permeabilized with ice-cold methanol for 10 min at −20 °C. After blocking non-specific sites with 2% BSA, cells were stained with mouse monoclonal anti-α-tubulin antibody (1:300 dilution in 2% BSA) for 2 h at 37 °C followed by Alexa 568 conjugated sheep antimouse IgG antibody (1:100 dilution in 2% BSA) for 1 h at 37 °C, to visualize microtubules. To visualize nuclei and DNA, cells were stained with 1 μg/ml 4, 6-diamidino-2-phenylindole (DAPI) for 20 s at 37 °C. Cells were washed with 1 × PBS after all incubations. All the coverslips were mounted in 50% glycerol in PBS containing 1 mg/ml ascorbic acid and cells were examined with a Nikon Eclipse 2000-U fluorescence microscope and the images were analyzed with the Image-Pro Plus software.

4.3.4. Purification of goat brain tubulin. Goat brain tubulin was isolated by two cycles of polymerization and depolymerization in the presence of glutamate and 10% (v/v) DMSO in assembly buffer (25 mM Pipes, pH 6.8, 3 mM $MgSO_4$, 1 mM EGTA, and 1 mM GTP). Microtubule associated protein (MAP)-free tubulin was obtained by phosphocellulose chromatography. Protein concentration was measured by using Bradford reagent with bovine serum albumin (BSA) as a standard.[47]

4.3.5. Inhibition of tubulin assembly by 3b, 3e, 3g, and 1c: light scattering. Purified goat brain tubulin (1 mg/ml) was incubated in the absence and presence of **3b**, **3e**, **3g**, and **1c** in assembly buffer containing 1 M sodium glutamate for 10 min at 0 °C. Polymerization was initiated by keeping the reaction mixture at 37 °C in a water bath. The rate and extent of polymerization was monitored by light scattering at 550 nm for 30 min in a JASCO FP 6500 fluorescence spectrophotometer using a 0.3 cm path length cuvette. The excitation and emission band passes were 5 and 10 nm, respectively. Buffer blank values were subtracted from all the measurements.

4.3.6. Transmission electron microscopy. Tubulin (1 mg/ml) was polymerized in the absence and presence of different concentrations (10 and 25 μM) of **3b**, **3e**, **3g**, and **1c** in assembly buffer as described above. The polymers were fixed with 0.5% glutaraldehyde for 10 min at 37 °C. Samples (40 μl) were applied to carbon coated electron microscope grids (300 mesh) for 15 s and blotted dry. The grids were negatively stained with 0.5% uranyl acetate solution for 45 s and air-dried. The samples were viewed in a Tecnai G^2 120 KV transmission electron microscope. Images were taken at 16500× magnification.

4.3.7. Binding measurements. Binding of **3b**, **3e**, **3g**, and **1c** to goat brain tubulin was determined by measuring the intrinsic tryptophan fluorescence quenching of tubulin.[39] To specifically excite the tryptophan residues in the tubulin, 295 nm was selected as the excitation wavelength. Tubulin (1 μM) was incubated with different concentrations (0–25 μM) of **3b**, **3e**, **3g**, and **1c** in PEM buffer (25 mM Pipes, pH 6.8, 3 mM $MgSO_4$, 1 mM EGTA) for 30 min at room temperature. Fluorescence measurements were taken in a JASCO FP-6500 spectrofluorometer using a 0.3 cm path length cuvette with excitation and emission wavelengths of 295 and 335 nm, respectively. Corrections due to the inner filter effects were made according to the formula $F = F_{OBS} \times \text{antilog}\ [(A_{EX} + A_{EM})/2]$, where A_{EX} is the absorbance of tryptophan at the excitation wavelength and A_{EM} is the absorbance of tryptophan at the emission wavelength. The fraction of binding sites (X) occupied by compounds **3b**, **3e**, **3g**, and **1c** was determined using the equation $X = (F - F_O)/F_{MAX}$, where F_O is the fluorescence intensity of tubulin in the absence of the tested compounds, F is the corrected fluorescence intensity of tubulin in the presence of **3b**, **3e**, **3g**, and **1c** and F_{MAX} was calculated from the plot of $1/(F - F_O)$ versus 1/[**3b**, **3e**, **3g**, and **1c**] and extrapolating 1/[**3b**, **3e**, **3g**, and **1c**] to zero. The dissociation constant (K_d) was determined using the relationship, $1/\alpha = 1 + K_d/L_F$, where L_F represents the free concentration of **3b**, **3e**, **3g**, and **1c** and α represents the concentration of **3b**, **3e**, **3g**, and **1c** that is bound to tubulin. $L_F = C - \alpha$ [Y], where C is the total concentration of **3b**, **3e**, **3g**, and **1c** and [Y] is the molar concentration of ligand binding sites assuming a single binding site per tubulin dimer. Data are an average of five independent experiments. The molar extinction coefficients for the compounds **3b**, **3e**, **3g**, and **1c** were determined to be 4820 ± 227, 5050 ± 398, 3888 ± 136, and 4144 ± 419 $M^{-1}\,cm^{-1}$ at 295 nm and 14893 ± 1329, 11888 ± 625, 6794 ± 136, and 6940 ± 210 $M^{-1}\,cm^{-1}$ at 335 nm, respectively.

4.3.8. Interaction of 3b, 3e, 3g, and 1c and ANS with tubulin. The change in 1-anilinonaphthalene-8-sulfonic acid (ANS) fluorescence at 470 nm upon binding to tubulin-MBH adduct complex was used to determine the interaction of **3b**, **3e**, **3g**, and **1c** with tubulin. Tubulin (1 μM) was incubated with varying concentrations (0–50 μM) of **3b**, **3e**, **3g**, and **1c** for 30 min at 25 °C. Forty micromolars ANS was added to the reaction mixtures and incubated for an additional 30 min at room temperature. The fluorescence measurements were performed with excitation wavelength of 400 nm and emission wavelength of 470 nm. Five independent experiments were performed.

4.3.9. Binding of vinblastine and MBH adducts 3b, 3e, 3g, and 1c to tubulin. Tubulin (3 μM) was first incubated with the vehicle DMSO, 100 μM vinblastine and 25 μM of **3b**, **3e**, **3g**, and **1c** at 37 °C for 45 min. Then, 2 μM fluorescent vinblastine (BODIPY FL-vinblastine) was added to all the mixtures and incubated for 20 min in dark at room temperature. Fluorescence spectra were collected with an excitation wavelength of 490 nm. The bound fluorescence spectra of tubulin–fluorescent vinblastine complex were obtained by subtracting the fluorescence spectra of unliganded fluorescent vinblastine in the absence of tubulin (blank spectra) from the spectra of fluorescent vinblastine in the presence of tubulin.

4.3.10. Kinetics of colchicine binding to tubulin. Tubulin (7 μM) was first incubated in the absence and presence of 25 μM of **3b**, **3e**, **3g**, and **1c** for 25 min at room temperature and then, 10 μM colchicine was added to the reaction mixtures. Fluorescence intensities were measured at different time points at 37 °C. The excitation and emission wavelengths were 360 and 430 nm, respectively. Corrections in fluorescence intensities because of the inner filter effects were made according to the formula $F_{corrected} = F_{OBS}$ X antilog $[(A_{EX} + A_{EM})/2]$, where A_{EX} is the absorbance of **3b**, **3e**, **3g**, and **1c** at the excitation wavelength and A_{EM} is the absorbance of **3b**, **3e**, **3g**, and **1c** at the emission wavelength. Data are the average of four independent experiments.

Colchicine binding to tubulin was also determined using the increase in the intrinsic fluorescence of colchicine when colchicine binds to tubulin.[46] Tubulin (7 μM) was first incubated with different concentrations (0, 5, 10, 25, and 50 μM) of **3b**, **3e**, **3g**, and **1c** for 30 min at 37 °C and then 10 μM colchicine was added to the reaction mixtures and further incubated for 60 min at 37 °C. The excitation and emission wavelengths were 360 and 430 nm, respectively.

Acknowledgments

This work was partly supported by a grant from the Department of Biotechnology, Government of India (to D. P. and I. N. N. N), partly by Swarnajayanti Fellowship (to D. P.), and a grant from CSIR, Government of India (to I. N. N. N.). R. M. thanks University Grant Commission, Government of India, and N. R. thanks IIT, Bombay, for a Fellowship. The authors thank SAIF, IIT Bombay, for NMR spectra and Dr. M. Cojocaru, Bar-Ilan University, Israel, for mass spectra.

Supplementary data

Supplementary data associated with this article can be found, in the online version, at doi:10.1016/j.bmc.2006.07.035.

References and notes

1. Recent reviews on nitro compounds: (a) Ballini, R.; Bosica, G.; Fiorini, D.; Palmieri, A.; Petrini, M. *Chem. Rev.* **2005**, *105*, 933; (b) Adams, J. P.; Box, D. S. *J. Chem. Soc., Perkin Trans.* **1999**, *1*, 749; (c) Luzzio, F. A. *Tetrahedron* **2001**, *57*, 915.
2. Recent reviews on conjugated nitroalkenes: (a) Berner, O. M.; Tedeschi, L.; Enders, D. *Eur. J. Org. Chem.* **2002**, 1877; (b) Krause, N.; Hoffmann-Röder, A. *Synthesis* **2001**, 171; (c) Denmark, S. E.; Thorarensen, A. *Chem. Rev.* **1996**, *96*, 137; (d) Tietze, L. F.; Kettschau, G. *Top. Curr. Chem.* **1997**, *189*, 1; see also: (e) Namboothiri, I. N. N.; Hassner, A. *Top. Curr. Chem.* **2001**, *216*, 1; (f) Namboothiri, I. N. N.; Ganesh, M.; Mobin, S. M.; Cojocaru, M. *J. Org. Chem.* **2005**, *70*, 2235.
3. Kabalka, G. W.; Varma, R. S. *Org. Prep. Proced. Int.* **1987**, *19*, 283, and the references cited therein.
4. Kamimura, A.; Noboru, O.; Tohei, T.; Hiroshi, K.; Hiroko, Y.; Kimitoshi, U.; Takao, I.; Tomohiro, T. *Jpn. Kokai Tokkyo Koho*. **1993**, JP 05139908; *Chem. Abstr.* **1993**, *119*, 133478.
5. (a) Gorska-Poczopko, J.; Grobelny, D.; Witek, S. *Organika* **1980**, 147; *Chem. Abstr*. **1981**, *95*, 475249; (b) Latif, N.; Guirguis, N. S.; Assad, F. M.; Grant, N. *Liebigs Ann.* **1985**, *12*, 1202, and the references cited therein.
6. (a) Latif, N.; Mishriky, N.; Guirguis, N. S.; Hussein, A. *J. Prakt. Chem.* **1973**, *315*, 419; (b) Latif, N.; Mishriky, N.; Guirguis, N. S.; Arnos, S. *Ind. J. Chem.* **1980**, *19B*, 301; (c) Latif, N.; Mishriky, N.; Assad, F. M.; Meguid, S. A. *Ind. J. Chem.* **1982**, *21B*, 872.
7. Blades, K.; Butt, A. H.; Cockerill, G. S.; Easterfield, H. J.; Lequeux, T. P.; Percy, J. M. *J. Chem. Soc., Perkin Trans.* **1999**, *1*, 3609.
8. Schultz, E. M.; Bicking, J. B.; Deana, A. A.; Gould, N. P.; Strobaugh, T. P.; Watson, L. S.; Cragoe, E. J., Jr. *J. Med. Chem.* **1976**, *19*, 783.
9. Nazarova, Z. N.; Potemkin, G. F. *Khimiko-Farmatsevticheskii Zhurnal* **1972**, *6*, 5; . *Chem. Abstr.* **1973**, *78*, 43166.
10. (a) Deshmukh, A. R. A. S.; Bhawal, B. M.; Shiralkar, V. P.; Rajappa, S. *Eur. Pat. Appl.* **1990**, 7; (b) *Chem. Abstr*. **1991**, *114*, 163525.
11. Hoashi, Y.; Yabuta, T.; Takemoto, Y. *Tetrahedron Lett.* **2004**, *45*, 9185.
12. (a) Morita, K.; Suzuki, Z.; Hirose, H. *Bull. Chem. Soc. Jpn.* **1968**, *41*, 2815; (b) Baylis, A. B.; Hillman, M. E. D. *Ger. Offen.* **1972**, DE 2155113. *Chem. Abstr.* **1972**, *77*, 434174. Hillman, M. E. D.; Baylis, A. B. U.S. Patent **1973**, US 3743669.
13. Reviews on MBH and related reactions: (a) Basavaiah, D.; Rao, A. J.; Satyanarayana, T. *Chem. Rev.* **2003**, *103*, 811; (b) Drewes, S. E.; Roos, G. H. P. *Tetrahedron* **1988**, *44*, 4653; (c) Basavaiah, D.; Rao, P. D.; Hyma, R. S. *Tetrahedron* **1996**, *52*, 8001; (d) Ciganek, E.. In *Organic Reactions*; Paquette, L. A., Ed.; John Wiley, 1997; Vol. 51, (e) Kataoka, T.; Kinoshita, H. *Eur. J. Org. Chem.* **2005**, 45.
14. For selected recent articles: (a) Price, K. E.; Broadwater, S. J.; Walker, B. J.; McQuade, D. T. *J. Org. Chem.* **2005**, *70*, 3980; (b) Yang, N.-F.; Gong, H.; Tang, W.-J.; Fan, Q.-H.; Cai, C.-Q.; Yang, L.-W. *J. Mol. Catal. A: Chem.* **2005**, *233*, 55; (c) Aggarwal, V. K.; Fulford, S. Y.; Lloyd-Jones, G. C. *Angew. Chem., Int. Ed.* **2005**, *44*, 1706; (d) Zhao, S.; Chen, Z. *Synth. Commun.* **2005**, *35*, 121; (e) Matsui, K.; Takizawa, S. *J. Am. Chem. Soc.* **2005**, *127*, 3680; (f) Lin, Y.-S.; Liu, C.-W.; Tsai, T. Y. R. *Tetrahedron Lett.* **2005**, *46*, 1859; (g) Mi, X.; Luo, S.; Cheng, J.-P. *J. Org. Chem.* **2005**, *70*, 2338; (h) Yadav, J. S.; Reddy, B. V. S.; Gupta, M. K.; Eeshwaraiah, B. *Synthesis* **2005**, 57; (i) Krishna, P. R.; Manjuvani, A.; Sekhar, E. R. *ARKIVOC* **2005**, 99; (j) Shi, M.; Chen, L.-H.; Li, C.-Q. *J. Am. Chem. Soc.* **2005**, *127*, 3790; (k) Kataoka, T.; Kinoshita, H. *Phosphorus, Sulfur Silicon Relat. Elem.* **2005**, *180*, 989; (l) Liu, X.; Zhao, J.; Jin, G.; Zhao, G.; Zhu, S.; Wang, S. *Tetrahedron* **2005**, *61*, 3841.
15. Baylis and Hillman in their original patent (Ref. 12b) have reported the reaction between nitroethylene and acetaldehyde in the presence of DABCO. However, no details or further reports on this or similar reactions are available.
16. Rastogi, N.; Namboothiri, I. N. N.; Cojocaru, M. *Tetrahedron Lett.* **2004**, *45*, 4745.
17. (a) Ballini, R.; Barboni, L.; Bosica, G.; Fiorini, D.; Mignini, E.; Palmieri, A. *Tetrahedron* **2004**, *60*, 4995, This report describes a reaction between aliphatic nitroalkenes and ethyl-2-bromomethylacrylate under the DBU catalyzed conditions, but the product is not a conjugated nitroalkene; For hydroxyalkylation of nitroalkenes with

activated non-enolizable carbonyl compounds: (b) Deb, I.; Dadwal, M.; Mobin, S. M.; Namboothiri, I. N. N. *Org. Lett.* **2006**, *8*, 1201; For hydrazination of conjugated nitroalkenes: (c) Dadwal, M.; Mobin, S. M.; Namboothiri, I. N. N. *Org. Biomol. Chem.* **2006**, *4*, 2525.

18. For recent selected references: (a) Felmer, R. N.; Clark, J. A. *Biol. Res.* **2004**, *37*, 449; (b) Akihisa, T.; Tokuda, H.; Ukiya, M.; Iizuka, M.; Schneider, S.; Ogasawara, K.; Mukainaka, T.; Iwatsuki, K.; Suzuki, T.; Nishino, H. *Cancer Lett.* **2003**, *201*, 133; (c) Khlebnikov, A.; Schepetkin, I.; Kim, B. S.; Kwon, B. S. In *Proceedings—KORUS 2001, the Korea-Russia International Symposium on Science and Technology*, 5th, Tomsk, Russian Federation, June 26–July 3, 2001; Vol. 3, Institute of Electrical and Electronics Engineers: New York, NY; (d) Papadopoulou, M. V.; Ji, M.; Rao, M. K.; Bloomer, W. D. *Oncol. Res.* **2001**, *12*, 185; (e) Sunel, V.; Basu, C.; Soldea, C.; Maftei-Sirbu, D. *Chimie* **1998**, *6*, 35; (f). *Chem. Abstr.* **2000**, *132*, 28756; (g) Breider, M. A.; Pilcher, G. D.; Graziano, M. J.; Gough, A. W. *Toxicol. Pathol.* **1998**, *26*, 234.
19. For the antitumor activity of aromatic nitroalkene against P-388 murine lymphocytic leukemia: (a) Cassels, B. K.; Herreros, S.; Ibanez, C.; Rezende, M. C.; Sebastian, C.; Sepulveda, S. *Anales de la Asociacion Quimica Argentina* **1982**, *70*, 283; (b). *Chem. Abstr.* **1982**, *97*, 400402; see also: (c) Zee-Cheng, K.-Y.; Cheng, C.-C. *J. Med. Chem.* **1969**, *12*, 157; (d) Pettit, R. K.; Hamel, E.; Verdier-Pinard, P.; Roberson, R. W.; Hazen, K. C.; Pettit, G. R.; Crews, L. C. *Mycoses* **2002**, *45*, 65.
20. For our recent reports on the preliminary studies on the anticancer properties of the Morita–Baylis–Hillman adducts of β-aryl nitroethylenes (a) with other activated alkenes: (a) Dadwal, M.; Mohan, R.; Panda, D.; Mobin, S. M.; Namboothiri, I. N. N. *Chem. Commun.* **2006**, 333; (b) with *N*-tosylimines: Rastogi, N.; Mohan, R.; Panda, D.; Mobin, S. M.; Namboothiri, I. N. N. *Org. Biomol. Chem.* **2006**, doi:10.1039/B607537A.
21. Hamel, E. *Med. Res. Rev.* **1996**, *16*, 207.
22. Jordan, M. A.; Wilson, L. *Nat. Rev. Cancer* **2004**, *4*, 253.
23. Wilson, L.; Jordan, M. A. *J. Chemother.* **2004**, *4*, 83.
24. Nicholson, K. M.; Phillips, R. M.; Shnyder, S. D.; Bibby, M. C. *Eur. J. Cancer* **2002**, *38*, 194.
25. Tew, K. D.; Hartley-Asp, B. *Urology* **1984**, *23*, 28.
26. Sangrajrang, S.; Denoulet, P.; Laing, N. M.; Tatoud, R.; Millot, G.; Calvo, F.; Tew, K. D.; Fellous, A. *Biochem. Pharmacol.* **1998**, *55*, 325.
27. Tinley, L. T.; Leal, M. R.; Randall-Hlibek, D. A.; Cessac, W. J.; Wilken, R. L.; Rao, N. P.; Mooberry, L. S. *Cancer Res.* **2003**, *63*, 1538.
28. Yokoi, A.; Kuromitsu, J.; Kawai, T.; Nagasu, T.; Sugi, H. N.; Yoshimatsu, K.; Yoshimo, H.; Owa, T. *Cancer Res.* **2003**, *63*, 1538.
29. Zhou, J.; Gupta, K.; Aggarwal, S.; Aneja, R.; Chandra, R.; Panda, D.; Joshi, C. H. *Mol. Pharmacol.* **2003**, *63*, 1.
30. (a) Muller, E.; Thieme, Ed.; Stuttgart. *Houben-Weyl: Methoden der Organische Chemie*, 1971, Vol. 10/1, p 9; (b) *Vogel's Text Book of Practical Organic Chemisty*, Addison Wesley Longman Ltd: Essex, England, 1996, p 1035.
31. For selected imidazole catalyzed MBH reactions: (a) Luo, S.; Wang, P. G.; Cheng, J.-P. *J. Org. Chem.* **2004**, *69*, 555; (b) Imbriglio, J. E.; Vasbinder, M. M.; Miller, S. *Org. Lett.* **2003**, *5*, 3741; (c) Gatri, R.; El Gaied, M. M. *Tetrahedron Lett.* **2002**, *43*, 7835; (d) Shi, M.; Jiang, Y. *J. Chem. Res.* **2003**, *12*, 564; (e) deSouza, R. O. M. A.; Vasconcellos, M. L. A. A. *Catal. Commun.* **2004**, *5*, 21.
32. (a) For proline co-catalyzed MBH reaction: (a) Ref. 31b; (b) Shi, M.; Jiang, J.-K.; Li, C.-Q. *Tetrahedron Lett.* **2002**, *43*, 127.
33. Selected X-ray crystallographic data for **3b** ($C_7H_7NO_3S$): space group = monoclinic P-2 1/n; *R* factor = 7.25; *a* = 11.56(14) lÅ; *b* = 5.12(9) Å; *c* = 13.89(15) Å; α = 90.00 deg; *β* = 106.15(9) deg; *γ* = 90.00; *V* = 789.60(19) Å^3; *Z* value = 4; D_{calcd} (g cm^{-1}) = 1.558; *λ* (Å) = 0.71073; *T* = 293(2) K. See also supporting information.
34. For selected recent reviews on organocatalysis: (a) Berkessel, A.; Groerger, H. *Asymmetric Organocatalysis*; Wiley-VCH Verlag GmbH: Weinheim, Germany, 2005; (b) Seayad, J.; List, B. *Org. Biomol. Chem.* **2005**, *3*, 719; (c) Dalko, P. I.; Moisan, L. *Angew. Chem., Int. Ed.* **2004**, *43*, 5138; (d) *Acc. Chem. Res.* **2004**, *37*, Spl. issue on organocatalysis; (e) Schreiner, P. R. *Chem. Soc. Rev.* **2003**, *32*, 289; (f) Jarvo, E. R.; Miller, S. J. *Tetrahedron* **2002**, *58*, 2481.
35. Gupta, K.; Bishop, J.; Peck, A.; Brown, J.; Wilson, L.; Panda, D. *Biochemistry* **2004**, *43*, 6645.
36. Panda, D.; Rathinasamy, K.; Santra, M. K.; Wilson, L. *Proc. Natl. Acad. Sci. U.S.A.* **2005**, *102*, 9878.
37. Gupta, K.; Panda, D. *Biochemistry* **2002**, *41*, 13029.
38. Hamel, A.; Lin, M. C. *Arch. Biochem. Biophys.* **1981**, *209*, 29.
39. Lee, C. J.; Harrison, D.; Timasheff, S. N. *J. Biol. Chem.* **1975**, *250*, 9272.
40. Bhattacharya, A.; Bhattacharyya, B.; Roy, S. *Protein Sci.* **1996**, *5*, 2029.
41. Panda, D.; Singh, J. P.; Wilson, L. *J. Biol. Chem.* **1997**, *272*, 7681.
42. Wood, L. D.; Panda, D.; Wiernicki, T. R.; Wilson, L.; Jordan, M. A.; Singh, J. P. *Mol. Pharmacol.* **1997**, *52*, 437.
43. Chatterjee, S. K.; Laffray, J.; Patel, P.; Ravindra, R.; Qin, Y.; Kuhne, E. M.; Bane, L. S. *Biochemistry* **2002**, *41*, 14010.
44. Bai, R. L.; Pettit, G. R.; Hamel, E. *J. Biol. Chem.* **1990**, *265*, 17141.
45. Wilson, L. *Biochemistry* **1970**, *9*, 4999.
46. Bhattacharya, B.; Wolff, J. *Proc. Natl. Acad. Sci. U.S.A.* **1974**, *71*, 2627.
47. Bradford, M. M. *Anal. Biochem.* **1976**, *72*, 248.